European Journal of Medicinal Chemistry 218 (2021) 113395

Contents lists available at ScienceDirect

European Journal of Medicinal Chemistry

journal homepage: http://www.elsevier.com/locate/ejmech

Flavonoid-triazolyl hybrids as potential anti-hepatitis C virus agents: Synthesis and biological evaluation

Han Zhang [a, 1], Xin Zheng [b, c, 1], Jichong Li [a], Qingbo Liu [a, **], Xiao-Xiao Huang [a], Huaiwei Ding [d, ***], Ryosuke Suzuki [c], Masamichi Muramatsu [c, ****], Shao-Jiang Song [a, *]

[a] Key Laboratory of Computational Chemistry Based Natural Antitumor Drug Research & Development, Liaoning Province, School of Traditional Chinese Materia Medica, Shenyang Pharmaceutical University, Shenyang, 110016, People's Republic of China
[b] Department of Cardiology, Third Affiliated Hospital of Guangzhou Medical University, Guangzhou, 510150, China
[c] Department of Virology II, National Institute of Infectious Diseases, 162-8640, Tokyo, Japan
[d] Key Laboratory of Structure-Based Drug Design and Discovery, Ministry of Education, Shenyang Pharmaceutical University, Shenyang, 110016, China

ARTICLE INFO

Article history:
Received 21 October 2020
Received in revised form
6 February 2021
Accepted 17 March 2021
Available online 31 March 2021

Keywords:
Flavonoid-triazolyl hybrids
Anti-HCV activity
HCV entry Inhibitors

ABSTRACT

A series of flavonoid-triazolyl hybrids were synthesized and evaluated as novel inhibitors of hepatitis C virus (HCV). The results of anti-HCV activity assays showed that most of the synthesized derivatives at a concentration of 100 μg/mL inhibited the generation of progeny virus. Among these derivatives, **10m** and **10r** exhibited the most potent anti-HCV activity and inhibited the production of HCV in a dose-dependent manner. Interestingly, **10m** and **10r** had no significant inhibitory effect on viral translation or replication. Additional action mechanism studies revealed that the most potent compounds, **10m** and **10r**, significantly inhibited viral entry to 34.0% and 52.0%, respectively, at 10 μM. These results suggest further effective application of **10m** and **10r** as potential HCV preventive agents.

1. Introduction

Hepatitis C virus (HCV) currently infects more than 180 million people globally, approximately 3% of the world population [1]. Annually, approximately 3 million people worldwide are newly infected with HCV, and more than 350,000 people die from HCV-related liver disease [2,3]. HCV is an enveloped, positive-sense single-stranded RNA virus belonging to the *Flaviviridae* family [4,5]. After infection, the HCV genome encodes a single polyprotein that can be cleaved by host and viral proteases into 10 kinds of viral proteins, including structural proteins (core, E1, and E2) and nonstructural proteins (NS2, NS3/4 A, NS4B, NS5A, and NS5B) [5]. NS3/4 A is a serine protease that is critical for cleaving four sites in the HCV polyprotein [6], as well as host factors such as interferon promoter stimulator-1 (IPS-1) [7]. The cleavage of viral proteins plays a very important role in virus replication and virus particle formation. Because it is essential for the viral life cycle, NS3-4 A is considered as a drug development target [8]. Although direct-acting antiviral (DAA) treatment can cure 90% of HCV-infection cases, this therapy is costly, especially in many upper-middle-income, high-income countries. Therefore, the development of more anti-HCV drugs is necessary.

Flavonoids represent a diverse group of natural polyphenols that are widely found in many medicinal plants, fungi and vegetables and possess various biological and pharmacological activities [9,10]. In particular, flavonoids have attracted increasing attention due to their inhibitory activity against several viruses, including HCV. Accumulating evidence has shown the ability of certain flavonoids to inhibit HCV propagation at different stages (Fig. 1) [11–13]. Additionally, several flavonoids, such as silymarin, have been proven to provide a beneficial and protective role in liver injury and fibrosis resulting from HCV infection [14,15]. Based on these therapeutic viewpoints, flavonoids seem to be promising scaffolds on which to build new derivatives with enhanced anti-HCV potency. Many studies have reported that the introduction of prenylated groups on a flavonoid skeleton can increase lipophilicity and endow the molecule with a high affinity towards biological membranes, leading to robust biological activity [16,17].

* Corresponding author.
** Corresponding author.
*** Corresponding author.
**** Corresponding author.
E-mail addresses: liuqingbolily@163.com (Q. Liu), dinghuaiwei627@163.com (H. Ding), muramatsu@niid.go.jp (M. Muramatsu), songsj99@163.com (S.-J. Song).
[1] These authors made equal contribution to the article.

https://doi.org/10.1016/j.ejmech.2021.113395
0223-5234/

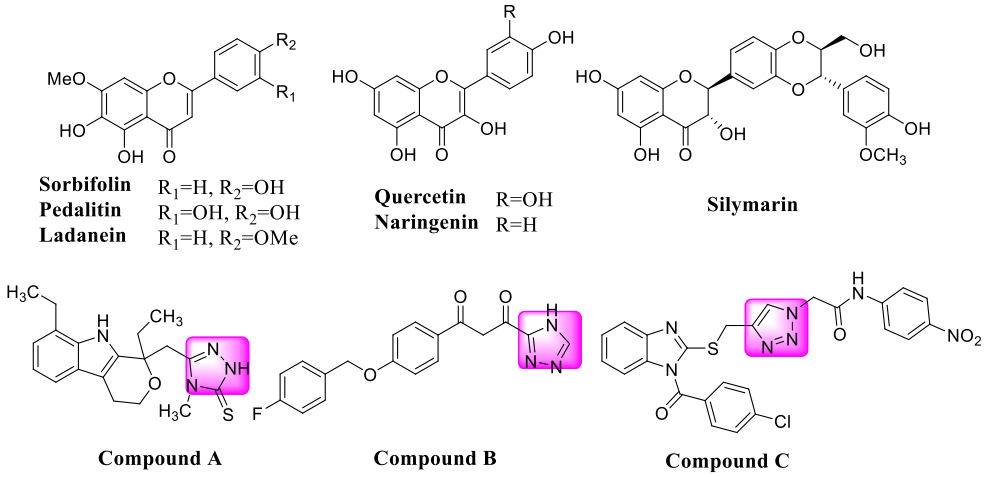

Fig. 1. Chemical structures of reported anti-HCV flavone compounds and anti-HCV compounds containing triazole moiety.

Furthermore, cyclization involving the prenylated group and the adjacent phenolic hydroxyl group of flavonoids to form pyranoflavonoids enhances bioactivities and decreases toxicity [18]. Inspired by these beneficial functions, a pyranoflavonoid was designed and totally synthesized as a chemical scaffold [19].

Triazole, one of the most important nitrogen heterocycles, can form various noncovalent interactions with different biological targets via hydrogen bonds, van der Waals interactions, hydrophobic interactions, or dipole-dipole bonds, which has wide applications in the pharmaceutical field and possesses diverse therapeutic properties [20–22]. Many studies have also shown that triazole-containing compounds (Fig. 1) possess anti-HCV effects [23–27], suggesting that the triazole moiety plays an intriguing role in the development of new anti-HCV agents. Therefore, different triazole groups were combined with the pyranoflavonoid scaffold to design a series of flavonoid derivatives as potential anti-HCV agents. All the designed compounds were evaluated for potential anti-HCV activity by using mCherry-NLS-IPS visualization system. In addition, the outstanding compound was selected for further evaluation of its inhibition of HCV progeny virus production and protein expression. Furthermore, assessments of their inhibitory effects on HCV replication and entry were also carried out to investigate the mode of action of the selected compounds against HCV.

2. Results and discussion

2.1. Chemistry

The synthetic route for flavanone and flavanone triazole hybrid synthesis is presented in Scheme 1. Compound **8** was prepared from 2,4-dihydroxyacetophenone (**1**) and *p*-hydroxybenzaldehyde (**3**). 2,4-Dihydroxyacetophenone was efficiently protected with methoxymethyl (MOM) chloride using K_2CO_3 in acetone to obtain 2,4-bis(methoxymethoxy)acetophenone (**2**) [28]. Compound **3** was alkylated with prenyl bromide to produce key intermediate **4** in a yield of 29.3%. Compound **4** was cyclized by using 2,3-dichloro-5,6-dicyano-1,4-benzoquinone (DDQ) to produce bicyclic intermediate **5**. The synthesis of chalcone **6** was based on a known methodology [29], and it was then cyclized using sodium acetate and deprotected with 3 N aqueous HCl to produce **8**. Then, compound **8** was reacted with bromopropyne in acetone in the presence of potassium carbonate to obtain intermediate **9**. Substituted azides were prepared from their corresponding halides with sodium azide in *N*,*N*-dimethylformamide (DMF) and used without further purification. Finally, a 1,3-dipolar cycloaddition reaction of intermediate **9** with these substituted azides in the presence of $CuSO_45H_2O$ and sodium L-ascorbate resulted in the formation of 1,4-substituted triazolyl derivatives **10a-10s** in yields of 55.8%—80.3%.

2.2. Biological evaluation

2.2.1. In vitro cytotoxic activity

The cytotoxic activity of all the synthesized flavonoid derivatives in initial screening was tested using Cell Proliferation Kit II (XTT). The toxicity of triazole-modified isopentenyl flavonoids (**10a**-**10s**) was generally lower than that of parent compound **8**, indicating that most of the derivatives were nontoxic to Huh7 cells (except compounds **10g** and **10j**) at 100 μg/mL (Fig. 2).

2.2.2. Establishment of the mCherry-NLS-IPS visualization system and initial screening

The HCV NS3/4 A protein cleaves the 508-cysteine of IPS-1 and then prevents the inhibition of viral proliferation [30]. In this study, based on the characteristics of the NS3/4 A protein, a visualization system was prepared by overexpressing the recombinant protein mCherry-NLS-IPS in Huh7 cells. In the absence of HCV infection, mCherry-NLS-IPS is localized on mitochondria, and the cytoplasmic region fluoresces red (Fig. 3). When Huh7 cells are infected, NS3/4 A cleaves the IPS-1 protein, and the nuclear localization sequence (NLS) sequence induces protein transfer from the cytoplasm into the nucleus, and then, the nuclear area fluoresce red [31].

The system enables a quick determination of whether the cells are infected with HCV. Therefore, it is suitable for screening antiviral drugs. Therefore, we used this system for the initial screening of all the prepared derivatives, and the results indicated that compounds **10d**, **10e**, **10m**, **10o** and **10r** showed significant HCV inhibitory activity (Fig. 4).

2.2.3. Inhibition of HCV progeny virus production and protein expression

The results of the preliminary screening showed that **10d**, **10e**, **10m**, **10o** and **10r** may effectively inhibit HCV infection. Subsequently, the supernatant of the HCV sample culture was harvested and used to reinfect Huh7 cells. After 48 h, HCV RNA in the reinfected cells was detected. The results showed that compounds **10d**, **10e**, **10m**, **10o** and **10r** at a concentration of 100 μg/mL had a significant inhibitory effect on the production of HCV progeny (Fig. 5).

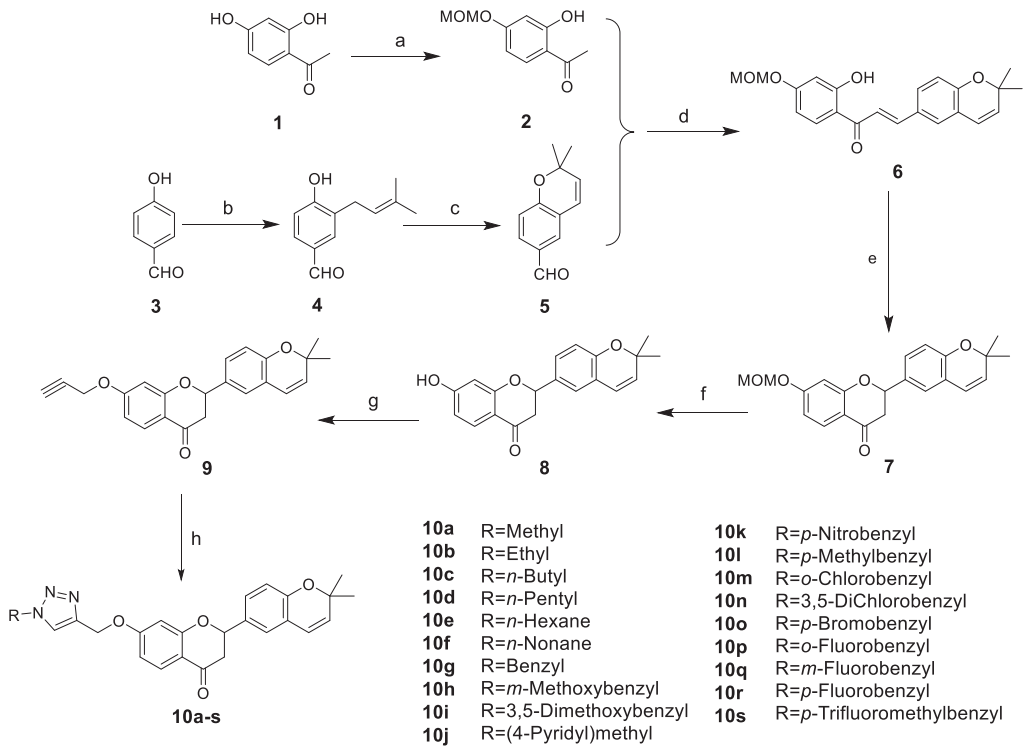

Scheme 1. Synthesis route of **8** and its derivatives. Reagents and conditions: (a) CH_3OCH_2Cl, K_2CO_3, acetone, reflux (b) prenyl bromide, KOH, r. t. (c) DDQ, toluene, reflux (d) KOH−H_2O−CH_3CH_2OH, ice-bath (e) CH_3CH_2OH/CH_3COONa, reflux (f) MeOH, dilute HCl (aq.) (g) K_2CO_3, acetone, reflux (h) $CuSO_45H_2O$, R−N_3, Na-*L*-ascorbate, *n*-butanol/H_2O (1:1).

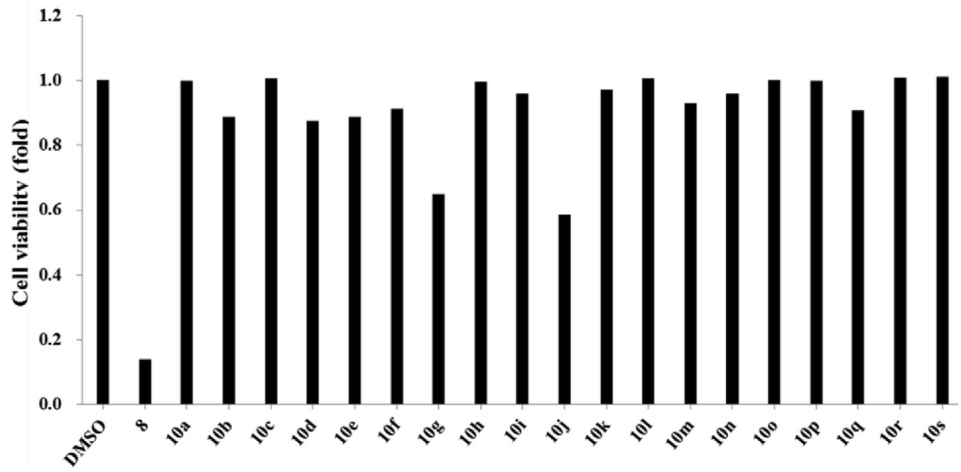

Fig. 2. Cell toxicity of selected compounds **8** and **10a**-**10s** were determined by Cell Proliferation Kit II (XTT). Huh7 cells were seeded per well overnight, treated with compounds (100 μg/mL) for 72 h before assessing toxicity by Cell Proliferation Kit II (XTT).

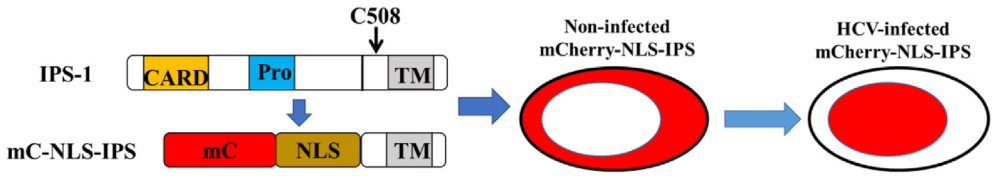

Fig. 3. Structural representation of IPS-1 denoting the aa positions of the CARD, Proline-rich region (Pro), transmembrane domain (TM), and the NS3/4 A cleavage site at C508.

Interestingly, the study found that the length of fatty side chains (**10d** and **10e**) can significantly affect this anti-HCV activity, with fatty acid chains that are too long or too short conferring the compound with a weaker antiviral effect. In addition, derivatives with aromatic side chains (**10m**, **10o** and **10r**) showed stronger antiviral activity than derivatives with fatty acid chains (**10d**, **10e**).

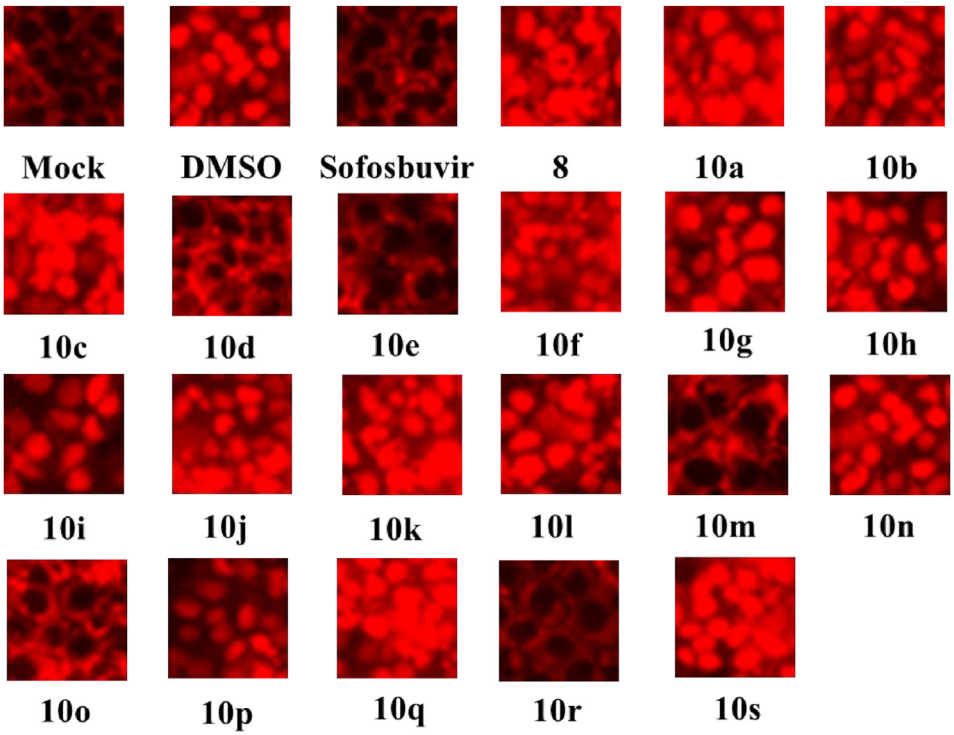

Fig. 4. The anti-HCV activity of parent compound **8** and all derivatives (**10a**-**10s**) was tested using the mCherry-NLS-IPS visualization system at a concentration of 100 μg/ml. Huh7-mCherry-NLS-IPS cells were infected with the HCV (JFH1). After 72 h of treatment, the change of the fluorescence signal in the cells was observed by using BZ-X710 KEYENCE.

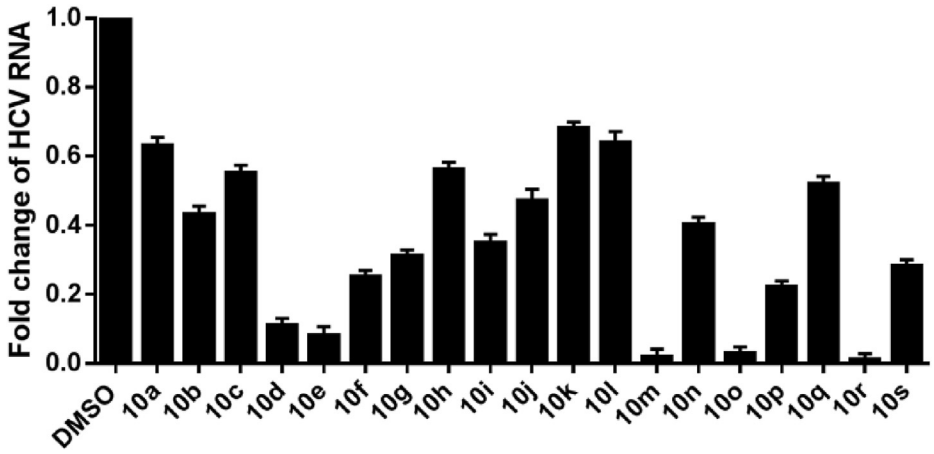

Fig. 5. Anti-HCV activity of synthetic derivatives in the supernatant. After treated Huh7-infected cells of each compound for 72 h, supernatant was harvested for reinfection to detect viral infectivity. Total RNA was extracted from reinfected Huh7 cells and subjected to RT-PCR for HCV 5′-UTR region to detect the level of viral RNA.

In summary, compared with parent compound **8**, the introduction of triazole fragments can reduce the toxicity of a compound and improve its antiviral activity as well as prevent HCV infection to a certain extent.

To confirm the anti-HCV effect of compounds **10m**, **10o** and **10r**, we treated Huh7 cells with compounds **10m**, **10o** and **10r** at the indicated concentrations (1 μM, 10 μM, 100 μM). Western blot assays were performed to determine the HCV protein expression levels. As shown in Fig. 6, treatment with these compounds resulted in a significant dose-dependent reduction in HCV protein expression compared to that in the control group (Fig. 6A).

Furthermore, after treatment with compounds **10m** and **10r** for 3 days (1 μM, 3 μM, 10 μM, 30 μM), HCV production was measured by the reinfection of Huh7 cells with the viral culture supernatant. Forty-eight hours after reinfection, HCV RNA was detected by RT-PCR, and IFNα (10U/mL) was used as a positive control (Fig. 6B). Both **10m** and **10r** have no or little cytotoxic activity. The results showed that compounds **10m** and **10r** exhibited potential anti-HCV activity with IC_{50} values of 5.285 μM and 9.004 μM, respectively. In addition, compounds **10m** and **10r** inhibited HCV production in a dose-dependent manner. At the concentration of 30 μM, the inhibitory effects of compounds **10m** and **10r** are comparable to the positive drug (10U/mL).

*2.2.4. Selected compounds **10m** and **10r** have no effect on HCV replication*

Antiviral compounds routinely target specific steps of the virus lifecycle, including attachment, entry, replication or assembly [32,33]. Our data showed that compounds **10m** and **10r** were active against HCV protein expression and progeny virus production after

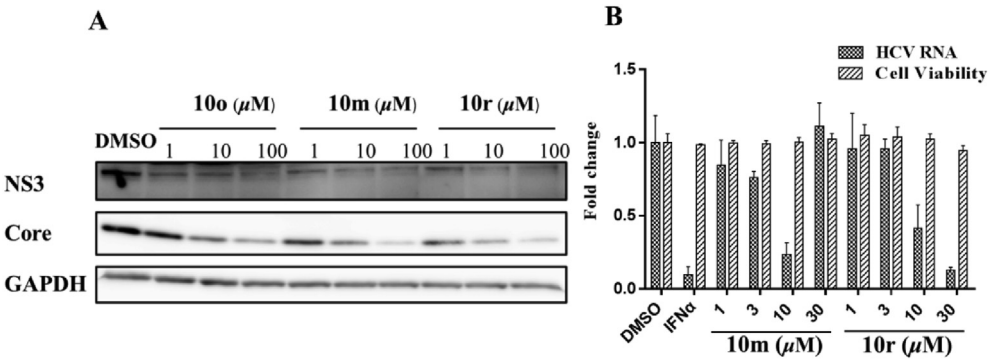

Fig. 6. Inhibitory effect on viral protein expression and infectivity. (A) NS3 and Core protein expression. Huh7 cells were treated with compounds at indicated concentrations, and the cell lysate was subjected to Western blotting with anti-NS3, anti-Core and anti-GAPDH antibodies. (B) Supernatant was harvested to reinfect Huh7 cells and test viral infectivity. Total RNA was extracted from reinfected cells and subjected to RT-PCR to detect HCV RNA. Data is presented as the mean ± SD of 3 independent experiments. $*P < 0.05$, $**P < 0.01$, and $***P < 0.001$ compared with the positive drug.

the HCV attachment step. Therefore, we preliminarily speculated that these compounds have a high probability of inhibiting processes after HCV attachment, including entry, translation, or replication.

To further investigate the mechanism of action of compound and evaluate their antiviral effect on HCV infection, a subgenomic construct (SGR-Luc-JFH1) based on the HCV JFH1 backbone was used to assess HCV replication (Fig. 7A) [34,35]. The results are shown in Fig. 7B. Compared with the level of the control group, there was no significant decrease in the luciferase signal after 10 μM treatment for 3 days, indicating that **10m** and **10r** did not suppress viral translation or replication. These results led us to speculate that the two compounds may target the HCV entry step, such as inhibiting internalization.

2.2.5. The inhibitory effect of selected compounds on HCV entry

Viral entry includes attachment and internalization that is considered as another target for the development of antiviral drugs [7]. If virus entry can be effectively blocked, it is possible to prevent cells from viral infection [36]. To confirm their mechanism, compounds **10m** and **10r** were investigated for their capacities to inhibit HCV entry using a HCV pseudo-particle (HCVpp) assay [37]. Huh7 cells were first treated with compounds **10m** and **10r** for 24 h and then infected with HCVpp. After 48 h, the cells were harvested to detect luciferase activity (Fig. 8A). Interestingly, our data suggested that compound pretreatment also inhibited the HCV entry step (Fig. 8B). Similarly, wild-type HCV was used for the pretreatment test. Huh7 cells were treated with **10m** and **10r** for 24 h, followed by HCV infection. HCV RNA was detected 48 h later. Our data suggested that **10m** and **10r** also somehow inhibited virus attachment in the pretreatment assay of both the HCVpp and wild-type infection systems (Fig. 8B and C), although **10m** and **10r** inhibited HCV infection more significantly during the post infection treatment (Fig. 6). All together, these results demonstrate that compounds **10m** and **10r** inhibit HCV production by targeting the HCV entry step, mainly HCV internalization.

The entry of HCV into cells represents the beginning of viral infection, which is essential for initiating viral infection and spread. In addition, viral entry is recognized as an important factor for graft reinfection and establishment of persistent infection. Preventing virus entry can effectively eradicate HCV infection before the viral cycle begins, and it may prevent the cell-to-cell transmission required for virus transmission [38]. Therefore, there is an urgent need for new antiviral prevention and treatment strategies.

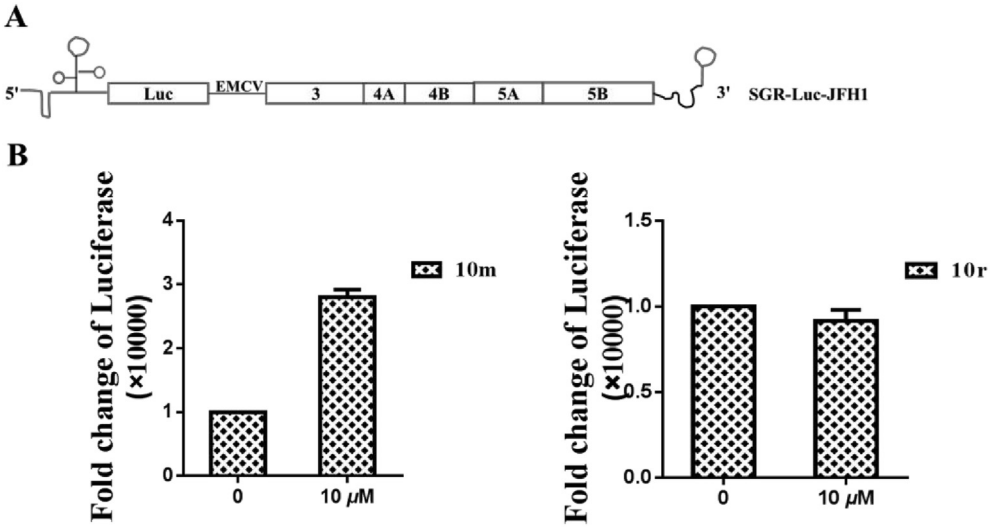

Fig. 7. 10m and **10r** do not inhibit HCV replication. (A) Subgenomic luciferase reporter gene JFH1 construct (SGR-Luc-JFH1) (not to scale). Luc, firefly luciferase gene; EMCV, EMCV IRES. (B) SGR was transfected to Huh7 cells, and then treated with **10m** or **10r**. Luciferase activity in cell extracts was measured after 72 h of incubation.

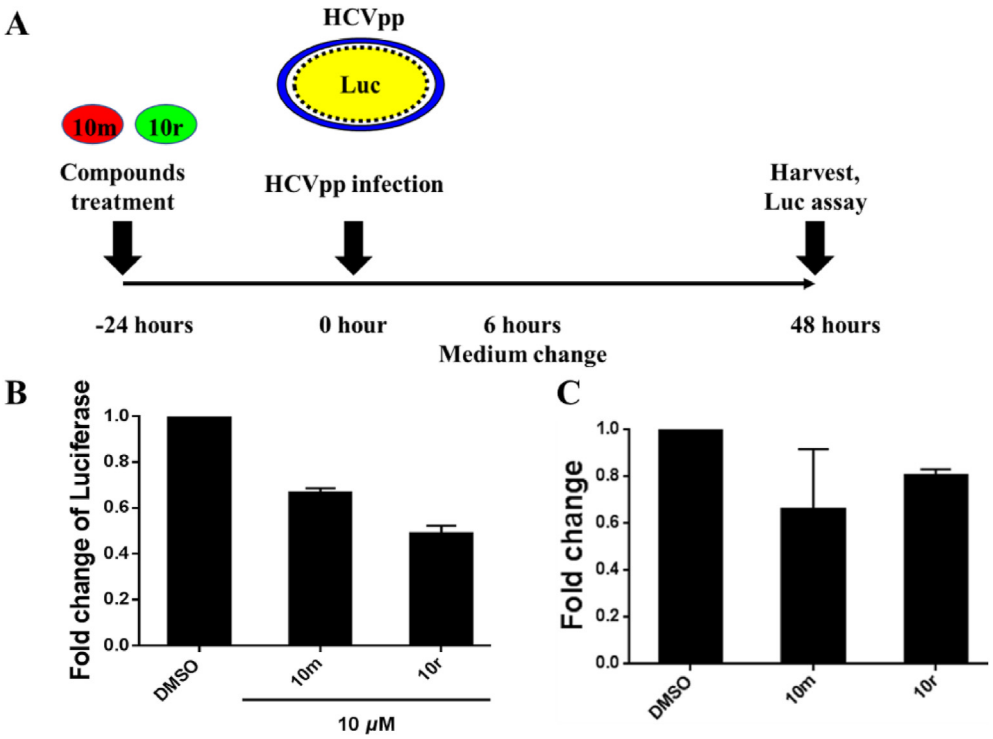

Fig. 8. (A) Schematic diagram of compound pre-treatment following with HCVpp infection. (B) **10m** and **10r** inhibited HCVpp entry. (C) The effect of pre-treatment with **10m** or **10r** during wildtype HCV infection.

Compounds **10m** and **10r** differ from other entry inhibitors reported in the literature in terms of structural type and from other marketed drugs in their mode of action (antiviral drugs currently on the market or being evaluated in clinical trials are mainly focused on targeting HCV nonstructural protein maturation or viral RNA synthesis). Therefore, compounds **10m** and **10r** represent a new class of anti-HCV entry inhibitors, and the results herein show that they can interfere with the internalization of HCV from the cell surface into the cell. Notably, the development of natural products into inhibitors can reduce costs, which increases the prospects for improving the approach to treatment, especially for countries or patients with limited resources [39]. In addition, entry inhibitors may have a synergistic effect with DAA, which may allow the use of small-dose combination regimens to reduce the cost and potential side effects of DAA [40,41]. More importantly, some reports suggested that DAA-resistance mutations in the HCV replication region were detected in HCV patients [42]. Current treatment options are limited by drug resistance, therefore the development of entry inhibitors plays an important role in HCV treatment. In summary, as a supplement to current treatment methods, HCV entry inhibitors represent a promising new class of antiviral drugs that can target the early steps of the viral life cycle.

3. Conclusion

By using a visualization anti-HCV compounds screening system, the potential anti-HCV effects of compounds **10m**, **10o** and **10r** were revealed. Furthermore, these compounds inhibited viral protein expression and de novo virus production in a dose-dependent manner. However, treatment with **10m** or **10r** did not significantly decrease the HCV subgenomic replicon system. It is suggested that these compounds did not contribute to the inhibition of HCV replication. Therefore, we speculated that by regulating the intracellular environment, the compounds inhibited the entry of viruses attaching to the cell surface. We employed the HCVpp model to confirm that whether HCV entry can be inhibited by these compounds. As expected, our data showed that compounds **10m** and **10r** inhibited virus entry by 34.0% and 52.0%, respectively, at noncytotoxic concentrations. These results indicated that **10m** and **10r** may be potential HCV entry inhibitors that exhibit effective antiviral activity and prevent HCV infections. In the future, they can be used in combination with therapeutic drugs at different stages or with different targets in the HCV infection cycle to establish new therapeutic methods.

4. Experimental protocols

4.1. Chemistry

4.1.1. General

Solvents and reagents were purchased from commercial sources and used without further purification. ^{1}H NMR and ^{13}C NMR spectra were measured on a Bruker ARX-400 or Bruker AVIII-600 spectrometer in DMSO-d_6 or $CDCl_3$. Mass spectra data were recorded with a Bruker Micro-TOF-Q instrument. The thin-layer chromatography (TLC) analysis was conducted on HSGF254 precoated silica gel plates (Yantai Zifu Chemical Group Co., China). Silica gel (Qingdao city, China) was used for column chromatography. The purity (%) of compounds was evaluated by high-performance liquid chromatography (HPLC, Agilent 1260 pump system) equipped with UV detector (Agilent 1260 detector) using Shodex ODS-A column (250 mm × 4.6 mm, 5 μm).

4.1.2. 1-(2-hydroxy-4-(methoxymethox)phenyl) ethan-1-one (2)

To a solution of 2,4-dihydroxyacetophenone (15.0 g, 0.10 mol) in dry acetone (60 mL) was added anhydrous K_2CO_3 (10.0 g, 0.07 mol) and stirred under reflux for 15 min. Methoxymethyl (MOM) chloride (7.6 mL, 0.105 mol) was added, and stirring at room

temperature continued for 15 min. Then, the mixture was refluxed for 2 h. The reaction was quenched with H_2O (60 mL) and extracted with CH_2Cl_2 (3 × 20 mL). The combined organic layers were washed with brine (60 mL), dried over anhydrous Na_2SO_4, and concentrated *in vacuo*. The crude product obtained was column chromatographed on silica gel eluting with petroleum ether/ethyl acetate (35:1) to afford compound **2** (17.0 g, 92.1% yield, obtained as white oil). ^{1}H NMR (600 MHz, $CDCl_3$, δ): 12.58 (1H, s), 7.60 (1H, d, J = 8.8 Hz), 6.54 (1H, d, J = 2.4 Hz), 6.50 (1H, dd, J = 8.8, 2.4 Hz), 5.16 (2H, s), 3.43 (3H, s), 2.51 (3H, s). The ^{1}H NMR data are consent with reference [29].

4.1.3. 4-Hydroxy-3-(3-methylbut-2-enyl) benzaldehyde (4)

4-hydroxybenzaldehyde (100.0 g, 0.82 mol) was dissolved in 150 mL aqueous potassium hydroxide (180.0 g, 3.21 mol) solution at ice water bath. To the solution was added 3,3-dimethylallyl bromide (170.0 g, 1.14 mol) and 150 mL aqueous potassium hydroxide (180.0 g, 3.21 mol) in parallel over 2 h with vigorous stirring. After the complete addition, the temperature was lowered to 25 °C, and the reaction was continued for 24 h in the dark. The reaction mixture was adjusted to pH 2 by addition of 3 N aqueous HCl. The reaction was extracted with EtOAc (3 × 40 mL). The combined organic layers were washed with 100 mL brine, dried over anhydrous Na_2SO_4, and concentrated *in vacuo*. The residue was chromatographed on silica gel with petroleum ether/ethyl acetate (4:1) to afford **4** (31.2 g, 20.5% yield, obtained as red-brown oil). ^{1}H NMR (600 MHz, $CDCl_3$, δ): 9.84 (1H, s, CHO), 7.67 (2H, overlap), 6.93 (1H, d, J = 8.1 Hz), 5.33 (1H, t, J = 7.3 Hz), 3.42 (2H, d, J = 7.3 Hz), 1.79 (3H, s), 1.78 (3H, s).

4.1.4. 2,2-dimethyl-2H-chromene-6-carbaldehyde (5)

Compound **4** (31.2 g, 0.16 mol) and DDQ (37.2 g, 0.16 mol) were dissolved in toluene heated at reflux for 12 h. After reaction was completed, reaction mixture was cooled to room temperature. The precipitate was filtered and washed thoroughly with toluene. The aqueous layer was extracted with EtOAc (3 × 40 mL) and the combined organic layers were dried over anhydrous Na_2SO_4, filtered and concentrated under reduced pressure. The residue was purified on silica gel with petroleum ether/ethyl acetate (15:1) to afford **5** (13.1 g, 42.2% yield, obtained as red-brown oil). ^{1}H NMR (600 MHz, $CDCl_3$, δ): 9.80 (1H, s, CHO), 7.61 (1H, dd, J = 8.3, 2.1 Hz), 7.49 (1H, d, J = 2.1 Hz), 6.83 (1H, d, J = 8.3 Hz), 6.34 (1H, d, J = 9.9 Hz), 5.67 (1H, d, J = 9.9 Hz), 1.44 (6H, s).

4.1.5. (E)-3-(2,2-dimethyl-2H-chromen-6-yl)-1-(2-hydroxy-4-(methoxymethoxy)phenyl)prop-2-en-1-one (6)

Compound **5** (13.1 g, 0.07 mol) was dissolved with compound **2** (13.6 g, 0.07 mol) in 50 mL ethanol. Under nitrogen and ice water bath, KOH (7.8 g, 0.14 mol) - H_2O (53 mL) - EtOH (80 mL) solution was slowly added dropwise over 1.5 h. Then it returned to room temperature and the reaction was continued for 24 h. Upon completion of reaction as monitored by TLC, the reaction mixture was washed with ethyl acetate three times (3 × 40 mL). The organic extract was washed with 50 mL water followed by 50 mL brine and dried over Na_2SO_4 and concentrated under vacuum. The residue was chromatographed on silica gel with petroleum ether/ethyl acetate (25:1) to afford **6** (13.4 g, 50.0% yield, obtained as yellowish oil). ^{1}H NMR (600 MHz, $CDCl_3$, δ): 13.40 (1H, s, HO), 7.83 (2H, overlap), 7.43 (2H, overlap), 7.28 (1H, d, J = 2.1 Hz), 6.81 (1H, d, J = 8.3 Hz), 6.64 (1H, d, J = 2.4 Hz), 6.58 (1H, dd, J = 8.9, 2.4 Hz), 6.36 (1H, d, J = 9.8 Hz), 5.68 (1H, d, J = 9.8 Hz), 5.22(2H, s), 3.49 (3H, s), 1.46 (6H, s).

4.1.6. 2-(2,2-dimethyl-2H-chromen-6-yl)-7-(methoxymethoxy) chroman-4-one (7)

Compound **6** (13.4 g, 0.04 mol) and sodium acetate (1.5 g, 0.02 mol) were added to 30 mL EtOH. The solution was heated to 70 °C for 12 h. After cooling to room temperature, the mixture was filtered. The solid was washed with 25 mL EtOAc, and the combined organic phases were concentrated under *vacuum*. The residue was chromatographed on silica gel with petroleum ether/ethyl acetate (40:1) to afford **7** (10.7 g, 80.1% yield, obtained as yellowish oil). ^{1}H NMR (600 MHz, $CDCl_3$, δ): 7.87 (1H, d, J = 8.7 Hz), 7.19 (1H, dd, J = 8.3, 2.3 Hz), 7.09 (1H, d, J = 2.2 Hz), 6.81 (1H, d, J = 8.2 Hz), 6.70 (1H, dd, J = 8.7, 2.3 Hz), 6.68 (1H, d, J = 2.3 Hz), 6.33 (1H, d, J = 9.8 Hz), 5.65 (1H, d, J = 9.8 Hz), 5.35 (1H, dd, J = 13.5, 2.8 Hz), 5.20 (1H, s), 3.47 (3H, s), 3.04 (1H, dd, J = 16.8, 13.5 Hz), 2.79 (1H, dd, J = 16.8, 2.8 Hz), 1.44 (6H, s).

4.1.7. 2-(2,2-dimethyl-2H-chromen-6-yl)-7-hydroxychroman-4-one (8)

To a solution of **7** (10.7 g, 0.03 mol) in MeOH (100 mL), 3 N aqueous HCl (8 mL) was added and the reaction mixture was stirred at 50 °C. After 12 h stirring, evaporated solvent under reduced pressure and quenched reaction mixture in 100 mL water. Extracted the mixture with EtOAc (3 × 40 mL) and organic layer was dried over anhydrous Na_2SO_4 and evaporated solvent to get the product. The crude product obtained was subjected to silica gel column chromatography and on elution with 10% ethyl acetate in hexane afforded the pure product (8.5 g, 90.5% yield, obtained as yellowish oil). ^{1}H NMR (600 MHz, $CDCl_3$, δ): 7.82 (1H, d, J = 8.6 Hz), 7.18 (1H, dd, J = 8.3, 2.3 Hz), 7.07 (1H, d, J = 2.2 Hz), 6.80 (1H, d, J = 8.2 Hz), 6.53 (1H, dd, J = 8.6, 2.3 Hz), 6.42 (1H, d, J = 2.3 Hz), 6.33 (1H, d, J = 9.8 Hz), 5.65 (1H, d, J = 9.8 Hz), 5.33 (1H, dd, J = 13.4, 3.0 Hz), 3.03 (1H, dd, J = 16.8, 13.4 Hz), 2.77 (1H, dd, J = 16.8, 2.9 Hz), 1.44 (6H, s).

4.1.8. General procedure for the synthesis of intermediate 9

To a solution of **8** (8.5 g, 0.03 mol) in dry acetone (30 mL) were added anhydrous K_2CO_3 (8.3 g, 0.06 mol) and bromopropyne (5.4 g, 0.045 mol). The solution was refluxed until TLC showed complete disappearance of the starting material (12 h). After cooling, acetone was removed under reduced pressure. The mixture was then extracted with 30 mL dichloromethane. The organic layer was washed with 30 mL H_2O and 30 mL brine, dried over Na_2SO_4, and concentrated *in vacuo*. The crude product obtained was subjected to silica gel column chromatography and on elution with petroleum ether/ethyl acetate (6:1) afforded pure product (8.2 g, 86.3% yield, obtained as yellowish oil). ^{1}H NMR (600 MHz, $CDCl_3$, δ): 7.88 (1H, d, J = 8.8 Hz), 7.20 (1H, dd, J = 8.3, 2.2 Hz), 7.09 (1H, d, J = 2.2 Hz), 6.81 (1H, d, J = 8.3 Hz), 6.67 (1H, dd, J = 8.8, 2.4 Hz), 6.58 (1H, d, J = 2.4 Hz), 6.34 (1H, d, J = 9.8 Hz), 5.65 (1H, d, J = 9.8 Hz), 5.36 (1H, dd, J = 13.5, 2.8 Hz), 4.71 (2H, d, J = 2.4 Hz), 3.05 (1H, dd, J = 16.8, 13.5 Hz), 2.79 (1H, dd, J = 16.8, 2.8 Hz), 2.56 (1H, t, J = 2.4 Hz), 1.45 (6H, s).

4.1.9. General procedure for the synthesis of conjugates 10a-10s

To a solution of compound **9** (100.8 mg, 0.28 mmol) and the appropriate azide (0.72 mmol) in *n*-butanol (10 mL) and H_2O (10 mL) was added $CuSO_4{\cdot}5H_2O$ (180.0 mg, 0.72 mmol) and sodium L-ascorbate (280.0 mg, 1.43 mmol). The reaction was stirred for 24 h at room temperature, until TLC analysis revealed a total consumption of compound **9**. The mixture was diluted with water (20 mL), extracted three times with CH_2Cl_2 (15 mL). The combined organic extracts were washed with 20 mL brine, dried over Na_2SO_4, filtered, concentrated, and purified via silica gel chromatography (petroleum ether/ethyl acetate, 8:1) to yield the target compounds **10a-10s**. The structures of the compounds were defined via HRMS

and NMR data.

4.1.9.1. 2-(2,2-dimethyl-2H-chromen-6-yl)-7-((1-methyl-1H-1,2,3-triazol-4-yl)methoxy)chroman-4-one (10a). Yield 70.8% as a yellow oil. ^{1}H NMR (600 MHz, DMSO-d_6, δ): 8.19 (1H, s), 7.72 (1H, d, J = 8.8 Hz), 7.27 (1H, dd, J = 8.1, 2.3 Hz), 7.26 (1H, d, J = 2.3 Hz), 6.78 (1H, d, J = 8.1 Hz), 6.76 (1H, d, J = 2.4 Hz), 6.71 (1H, dd, J = 8.8, 2.4 Hz), 6.43 (1H, d, J = 9.8 Hz), 5.79 (1H, d, J = 9.8 Hz), 5.51 (1H, dd, J = 13.1, 2.8 Hz), 5.21 (2H, s), 4.05 (3H, s), 3.18 (1H, dd, J = 16.8, 13.2 Hz), 2.70 (1H, dd, J = 16.8, 2.9 Hz), 1.38 (6H, s). ^{13}C NMR (150 MHz, DMSO-d_6, δ): 190.7, 164.8, 163.6, 153.1, 142.5, 132.0, 131.6, 128.5, 128.3, 126.1, 125.5, 122.0, 121.3, 116.2, 115.1, 110.9, 102.3, 79.5, 76.8, 62.0, 43.5, 36.8, 28.2 × 2. ESI-HRMS: m/z 418.1765 $[M+H]^+$ (Calcd for $C_{24}H_{24}N_3O_4$, 418.1761). HPLC purity: 95.76%.

4.1.9.2. 2-(2,2-dimethyl-2H-chromen-6-yl)-7-((1-ethyl-1H-1,2,3-triazol-4-yl)methoxy)chroman-4-one (10b). Yield 55.8% as a yellow oil. ^{1}H NMR (600 MHz, DMSO-d_6, δ): 8.27 (1H, s), 7.72 (1H, d, J = 8.8 Hz), 7.27 (1H, dd, J = 8.2, 2.3 Hz), 7.26 (1H, d, J = 2.3 Hz), 6.80–6.70 (2H, overlap), 6.72 (1H, dd, J = 8.8, 2.4 Hz), 6.42 (1H, d, J = 9.8 Hz), 5.78 (1H, d, J = 9.8 Hz), 5.51 (1H, dd, J = 13.1, 2.8 Hz), 5.21 (2H, s), 4.39 (2H, q, J = 7.4 Hz), 3.18 (1H, dd, J = 16.8, 13.1 Hz), 2.71 (1H, dd, J = 16.8, 2.8 Hz), 1.43 (3H, t, J = 7.3 Hz), 1.38 (6H, s). ^{13}C NMR (150 MHz, DMSO-d_6, δ): 190.7, 164.8, 163.6, 153.1, 142.4, 131.9, 131.6, 128.5, 128.2, 125.5, 124.7, 122.0, 121.3, 116.2, 115.1, 110.8, 102.3, 79.5, 76.8, 62.1, 45.1, 43.5, 28.2 × 2, 15.8. ESI-HRMS: m/z 432.1920 $[M+H]^+$ (Calcd for $C_{25}H_{26}N_3O_4$, 432.1918). HPLC purity: 99.63%.

*4.1.9.3. 7-((1-butyl-1H-1,2,3-triazol-4-yl)methoxy)-2-(2,2-dimethyl-2H-chromen-6-yl)chroman-4-one (**10c**).* Yield 73.7% as a yellow oil. ^{1}H NMR (400 MHz, $CDCl_3$, δ): 7.99 (1H, s), 7.85 (1H, d, J = 8.8 Hz), 7.17 (1H, dd, J = 8.3, 2.3 Hz), 7.07 (1H, d, J = 2.3 Hz), 6.79 (1H, d, J = 8.3 Hz), 6.66 (1H, dd, J = 8.8, 2.4 Hz), 6.58 (1H, d, J = 2.4 Hz), 6.32 (1H, d, J = 9.8 Hz), 5.64 (1H, d, J = 9.8 Hz), 5.33 (1H, dd, J = 13.1, 2.8 Hz), 5.20 (2H, s), 4.35 (2H, t, J = 7.3 Hz), 3.02 (1H, dd, J = 16.8, 13.1 Hz), 2.77 (1H, dd, J = 16.8, 2.8 Hz), 1.88 (2H, m), 1.43 (6H, s), 1.35 (2H, m), 0.94 (3H, t, J = 7.4 Hz). ^{13}C NMR (100 MHz, $CDCl_3$, δ): 190.8, 164.7, 163.5, 153.4, 143.1, 131.4, 130.8, 128.8, 127.2, 124.4, 122.7, 121.9, 121.4, 116.5, 115.2, 110.5, 101.9, 79.8, 76.6, 62.3, 50.2, 44.0, 32.2, 28.1 × 2, 19.7, 13.4. ESI-HRMS: m/z 460.2227 $[M+H]^+$ (Calcd for $C_{27}H_{30}N_3O_4$, 460. 2231). HPLC purity: 90.82%.

4.1.9.4. 2-(2,2-dimethyl-2H-chromen-6-yl)-7-((1-pentyl-1H-1,2,3-triazol-4-yl)methoxy)chroman-4-one (10d). Yield 63.5% as a yellow oil. ^{1}H NMR (600 MHz, DMSO-d_6, δ): 8.25 (1H, s), 7.73 (1H, d, J = 8.8 Hz), 7.29–7.25 (2H, overlap), 6.80–6.76 (2H, overlap), 6.72 (1H, dd, J = 8.8, 2.4 Hz), 6.42 (1H, d, J = 9.8 Hz), 5.77 (1H, d, J = 9.8 Hz), 5.50 (1H, dd, J = 13.1, 2.8 Hz), 5.22 (2H, s), 4.35 (2H, t, J = 7.3 Hz), 3.16 (1H, dd, J = 16.8, 13.1 Hz), 2.71 (1H, dd, J = 16.8, 2.8 Hz), 1.81 (2H, m), 1.38 (6H, s),1.29 (2H, m), 1.20 (2H, m), 0.84 (3H, t, J = 7.3 Hz). ^{13}C NMR (150 MHz, DMSO-d_6, δ): 190.6, 164.8, 163.5, 153.1, 142.3, 131.9, 131.6, 128.5, 128.2, 125.4, 125.1, 122.0, 121.3, 116.2, 115.1, 110.8, 102.3, 79.5, 76.8, 62.1, 49.9, 43.5, 29.9, 28.5, 28.2 × 2, 22.0, 14.2. ESI-HRMS: m/z 474.2390 $[M+H]^+$ (Calcd for $C_{28}H_{32}N_3O_4$, 474.2387). HPLC purity: 98.72%.

*4.1.9.5. 2-(2,2-dimethyl-2H-chromen-6-yl)-7-((1-hexyl-1H-1,2,3-triazol-4-yl)methoxy)chroman-4-one (**10e**).* Yield 57.6% as a yellow oil. ^{1}H NMR (600 MHz, DMSO-d_6, δ): 8.26 (1H, s), 7.72 (1H, d, J = 8.8 Hz), 7.27 (1H, dd, J = 8.2, 2.3 Hz), 7.25 (1H, d, J = 2.3 Hz), 6.78 (1H, d, J = 8.2 Hz), 6.76 (1H, d, J = 2.4 Hz), 6.71 (1H, dd, J = 8.8, 2.4 Hz), 6.43 (1H, d, J = 9.8 Hz), 5.78 (1H, d, J = 9.8 Hz), 5.51 (1H, dd, J = 13.1, 2.8 Hz), 5.21 (2H, s), 4.36 (2H, t, J = 7.3 Hz), 3.17 (1H, dd, J = 16.8, 13.1 Hz), 2.70 (1H, dd, J = 16.8, 2.8 Hz), 1.80 (2H, m), 1.41 (3H, s), 1.38 (3H, s), 1.25–1.15 (6H, overlap), 0.82 (3H, t, J = 7.3 Hz). ^{13}C NMR (150 MHz, DMSO-d_6, δ): 190.7, 164.8, 163.5, 153.1, 142.3, 131.9, 131.6, 128.5, 128.2, 125.5, 125.1, 122.0, 121.3, 116.2, 115.1, 110.8, 102.3, 79.5, 76.8, 49.9, 43.5, 31.0, 30.1, 28.4, 28.2, 25.9, 22.4, 14.3. ESI-HRMS: m/z 488.2547 $[M+H]^+$ (Calcd for $C_{29}H_{34}N_3O_4$, 488.2544). HPLC purity: 98.04%.

*4.1.9.6. 2-(2,2-dimethyl-2H-chromen-6-yl)-7-((1-nonyl-1H-1,2,3-triazol-4-yl)methoxy)chroman-4-one (**10f**).* Yield 67.9% as a yellow oil. ^{1}H NMR (600 MHz, DMSO-d_6, δ): 8.24 (1H, s), 7.72 (1H, d, J = 8.8 Hz), 7.27 (1H, dd, J = 8.2, 2.3 Hz), 7.25 (1H, d, J = 2.3 Hz), 6.78 (1H, d, J = 8.2 Hz), 6.76 (1H, d, J = 2.4 Hz), 6.71 (1H, dd, J = 8.8, 2.4 Hz), 6.42 (1H, d, J = 9.8 Hz), 5.77 (1H, d, J = 9.8 Hz), 5.50 (1H, dd, J = 13.1, 2.8 Hz), 5.21 (2H, s), 4.35 (2H, t, J = 7.3 Hz), 3.16 (1H, dd, J = 16.8, 13.1 Hz), 2.70 (1H, dd, J = 16.8, 2.8 Hz), 1.79 (2H, m), 1.38 (6H, s), 1.27–1.17 (12H, overlap), 0.83 (3H, t, J = 7.3 Hz). ^{13}C NMR (150 MHz, DMSO-d_6, δ): 190.6, 164.8, 163.5, 153.1, 142.3, 131.9, 131.6, 128.5, 128.2, 125.4, 125.1, 122.0, 121.3, 116.2, 115.1, 110.8, 102.3, 79.5, 76.8, 62.1, 49.9, 43.5, 31.7, 30.2, 29.3, 29.1, 28.9, 28.2 × 2, 26.3, 22.6, 14.4. ESI-HRMS: m/z 530.3019 $[M+H]^+$ (Calcd for $C_{32}H_{40}N_3O_4$, 530. 3013). HPLC purity: 96.04%.

*4.1.9.7. 7-((1-benzyl-1H-1,2,3-triazol-4-yl)methoxy)-2-(2,2-dimethyl-2H-chromen-6-yl)chroman-4-one (**10g**).* Yield 80.3% as a yellow oil. ^{1}H NMR (600 MHz, DMSO-d_6, δ): 8.31 (1H, s), 7.71 (1H, d, J = 8.8 Hz), 7.40–7.30 (5H, Ar–H, overlap), 7.27 (2H, overlap), 6.79 (1H, d, J = 8.2 Hz), 6.76 (1H, d, J = 2.4 Hz), 6.71 (1H, dd, J = 8.8, 2.4 Hz), 6.43 (1H, d, J = 9.8 Hz), 5.79 (1H, d, J = 9.8 Hz), 5.61 (2H, s), 5.51 (1H, dd, J = 13.1, 2.8 Hz), 5.21 (2H, s), 3.18 (1H, dd, J = 16.8, 13.1 Hz), 2.69 (1H, dd, J = 16.8, 2.8 Hz), 1.38(6H, s). ^{13}C NMR (150 MHz, DMSO-d_6, δ): 190.7, 164.8, 163.6, 153.1, 142.7, 136.4, 132.0, 131.6, 129.2 × 2, 128.7, 128.5, 128.4 × 2, 128.3, 125.5, 125.4, 122.0, 121.3, 116.2, 115.1, 110.9, 102.3, 79.5, 76.8, 62.0, 53.3, 43.5, 28.2 × 2. ESI-HRMS: m/z 494. 2104 $[M+H]^+$ (Calcd for $C_{30}H_{28}N_3O_4$, 494.2094). HPLC purity: 90.76%.

*4.1.9.8. 2-(2,2-dimethyl-2H-chromen-6-yl)-7-((1-(3-methoxybenzyl)-1H-1,2,3-triazol-4-yl)methoxy)chroman-4-one (**10h**).* Yield 70.2% as a yellow oil. ^{1}H NMR (400 MHz, DMSO-d_6, δ): 8.31 (1H, s), 7.71 (1H, d, J = 8.8 Hz), 7.30–7.25 (3H, overlap), 6.92–6.85 (3H, overlap), 6.80–6.75 (2H, overlap), 6.71 (1H, dd, J = 8.8, 2.4 Hz), 6.43 (1H, d, J = 9.8 Hz), 5.79 (1H, d, J = 9.8 Hz), 5.57 (2H,s), 5.51 (1H, dd, J = 13.1, 2.8 Hz), 5.21 (2H, s), 3.72 (3H, s), 3.18 (1H, dd, J = 16.8, 13.1 Hz), 2.69 (1H, dd, J = 16.8, 2.8 Hz), 1.38 (6H, s). ^{13}C NMR (100 MHz, DMSO-d_6, δ): 190.7, 164.8, 163.5, 159.9, 153.1, 142.7, 137.8, 132.0, 131.6, 130.4, 128.5, 128.3, 125.5, 125.4, 122.0, 121.3, 120.5, 116.2, 115.1, 114.2, 114.0, 110.9, 102.3, 79.5, 76.8, 62.0, 55.6, 53.2, 43.5, 28.2 × 2. ESI-HRMS: m/z 524.2194 $[M+H]^+$ (Calcd for $C_{31}H_{30}N_3O_5$, 524.2180). HPLC purity: 98.73%.

*4.1.9.9. 7-((1-(3,5-dimethoxybenzyl)-1H-1,2,3-triazol-4-yl)methoxy)-2-(2,2-dimethyl-2H-chromen-6-yl)chroman-4-one (**10i**).* Yield 76.5% as a yellow oil. ^{1}H NMR (400 MHz, DMSO-d_6, δ): 8.31 (1H, s), 7.71 (1H, d, J = 8.8 Hz), 7.26 (2H, overlap), 6.77 (2H, overlap), 6.71 (1H, dd, J = 8.8, 2.4 Hz), 6.46 (3H, overlap), 6.43 (1H, d, J = 9.8 Hz), 5.79 (1H, d, J = 9.8 Hz), 5.52 (2H, s), 5.50 (1H, dd, J = 13.1, 2.8 Hz), 5.21 (2H, s), 3.70 (6H, s), 3.18 (1H, dd, J = 16.8, 13.1 Hz), 2.69 (1H, dd, J = 16.8, 2.8 Hz), 1.38 (6H, s). ^{13}C NMR (100 MHz, DMSO-d_6, δ): 190.7, 164.7, 163.5, 161.1 × 2, 153.1, 142.7, 138.5, 132.0, 131.6, 128.5, 128.3, 125.5, 125.4, 122.0, 121.3, 116.2, 115.1, 110.9, 106.6 × 2, 102.3, 100.1, 79.5, 76.8, 62.0, 55.7 × 2, 53.3, 43.5, 28.2 × 2. ESI-HRMS: m/z 554. 2285 $[M+H]^+$ (Calcd for $C_{32}H_{32}N_3O_6$, 554.2286). HPLC purity: 95.38%.

*4.1.9.10. 2-(2,2-dimethyl-2H-chromen-6-yl)-7-((1-(pyridin-4-ylmethyl)-1H-1,2,3-triazol-4-yl)methoxy)chroman-4-one (**10j**).*

Yield 69.3% as a yellow oil. ^{1}H NMR (400 MHz, DMSO-d_6, δ): 8.56 (2H, overlap), 8.38 (1H, s), 7.72 (1H, d, J = 8.8 Hz), 7.27 (1H, dd, J = 8.1, 2.3 Hz), 7.26 (1H, d, J = 2.3 Hz), 7.20 (2H, overlap), 6.78 (2H, overlap), 6.72 (1H, dd, J = 8.8, 2.4 Hz), 6.43 (1H, d, J = 9.8 Hz), 5.79 (1H, d, J = 9.8 Hz), 5.71 (2H, s), 5.51 (1H, dd, J = 13.1, 2.8 Hz), 5.24 (2H, s), 3.19 (1H, dd, J = 16.8, 13.1 Hz), 2.70 (1H, dd, J = 16.8, 2.8 Hz), 1.38 (6H, s). ^{13}C NMR (100 MHz, DMSO-d_6, δ): 190.7, 164.7, 163.6, 153.1, 150.5 × 2, 145.2, 142.9, 132.0, 131.6, 128.5, 128.3, 126.0, 125.5, 122.8 × 2, 122.0, 121.3, 116.2, 115.1, 110.9, 102.3, 79.5, 76.8, 62.0, 52.0, 43.5, 28.2 × 2. ESI-MS: m/z 495.3 $[M+Na]^+$ (Calcd for $C_{29}H_{26}N_4O_4Na$, 495.2). HPLC purity: 99.41%.

*4.1.9.11. 2-(2,2-dimethyl-2H-chromen-6-yl)-7-((1-(4-nitrobenzyl)-1H-1,2,3-triazol-4-yl)methoxy)chroman-4-one (**10k**).* Yield 59.1% as a yellow oil. ^{1}H NMR (400 MHz, DMSO-d_6, δ): 8.39 (1H, s), 8.24 (2H, overlap), 7.72 (1H, d, J = 8.8 Hz), 7.54 (2H, overlap), 7.27 (1H, dd, J = 8.1, 2.3 Hz), 7.25 (1H, d, J = 2.3 Hz), 6.77 (2H, overlap), 6.72 (1H, dd, J = 8.8, 2.4 Hz), 6.42 (1H, d, J = 9.8 Hz), 5.81 (2H, s), 5.79 (1H, d, J = 9.8 Hz), 5.51 (1H, dd, J = 13.1, 2.8 Hz), 5.23 (2H, s), 3.19 (1H, dd, J = 16.8, 13.1 Hz), 2.70 (1H, dd, J = 16.8, 2.8 Hz), 1.38 (6H, s). ^{13}C NMR (100 MHz, DMSO-d_6, δ): 190.7, 164.7, 163.6, 153.1, 147.7, 143.8, 142.9, 132.0, 131.6, 129.6 × 2, 128.5, 128.3, 125.9, 125.5, 124.4 × 2, 122.0, 121.3, 116.2, 115.1, 110.9, 102.3, 79.5, 76.8, 62.0, 52.4, 43.5, 28.2 × 2. ESI-HRMS: m/z 539.1968 $[M+H]^+$ (Calcd for $C_{30}H_{27}N_4O_6$, 539.1965). HPLC purity: 99.45%.

*4.1.9.12. 2-(2,2-dimethyl-2H-chromen-6-yl)-7-((1-(4-methylbenzyl)-1H-1,2,3-triazol-4-yl)methoxy)chroman-4-one (**10l**).* Yield 58.8% as a yellow oil. ^{1}H NMR (400 MHz, DMSO-d_6, δ): 8.27 (1H, s), 7.71 (1H, d, J = 8.7 Hz), 7.20 (2H, overlap 7.04 (2H, overlap), 6.84–6.80 (2H, overlap), 6.78 (1H, d, J = 8.2 Hz), 6.76 (1H, d, J = 2.4 Hz), 6.71 (1H, dd, J = 8.7, 2.4 Hz), 6.42 (1H, d, J = 9.8 Hz), 5.79 (1H, d, J = 9.8 Hz), 5.75 (2H, s), 5.51 (1H, dd, J = 13.1, 2.8 Hz), 5.20 (2H, s), 3.16 (1H, dd, J = 16.8, 13.1 Hz), 2.69 (1H, dd, J = 16.8, 2.8 Hz), 2.27 (3H, s), 1.38 (6H, s). ^{13}C NMR (100 MHz, DMSO-d_6, δ): 190.7, 164.8, 163.5, 153.1, 142.7, 138.0, 133.4, 132.0, 131.6, 129.8, 129.7 × 2, 128.5 × 2, 128.2, 125.5, 125.3, 122.0, 121.3, 116.2, 115.1, 110.8, 102.3, 79.5, 76.8, 62.0, 53.1, 43.5, 28.2 × 2, 21.2. ESI-HRMS: m/z 508.2193 $[M+H]^+$ (Calcd for $C_{31}H_{30}N_3O_4$, 508.2201). HPLC purity: 98.75%.

*4.1.9.13. 7-((1-(2-chlorobenzyl)-1H-1,2,3-triazol-4-yl)methoxy)-2-(2,2-dimethyl-2H-chromen-6-yl)chroman-4-one (**10m**).* Yield 57.2% as a yellow oil. ^{1}H NMR (400 MHz, DMSO-d_6, δ): 8.29 (1H, s), 7.71 (1H, d, J = 8.7 Hz), 7.52 (1H, m), 7.38 (2H,overlap), 7.26 (3H, overlap), 6.78 (1H, d, J = 8.2 Hz), 6.77 (1H, d, J = 2.4 Hz), 6.71 (1H, dd, J = 8.7, 2.4 Hz), 6.43 (1H, d, J = 9.8 Hz), 5.79 (1H, d, J = 9.8 Hz), 5.72 (2H, s), 5.51 (1H, dd, J = 13.1, 2.8 Hz), 5.22 (2H, s), 3.19 (1H, dd, J = 16.8, 13.1 Hz), 2.69 (1H, dd, J = 16.8, 2.8 Hz), 1.38 (6H, s). ^{13}C NMR (100 MHz, DMSO-d_6, δ): 190.7, 164.7, 163.6, 153.1, 142.5, 133.6, 133.1, 132.0, 131.6, 131.0, 130.8, 130.1, 128.5, 128.3, 128.2, 125.9, 125.5, 122.0, 121.3, 116.2, 115.1, 110.9, 102.3, 79.5, 76.8, 62.0, 51.1, 43.5, 28.2 × 2. ESI-HRMS: m/z 528.1649 $[M+H]^+$ (Calcd for $C_{30}H_{27}ClN_3O_4$, 528.1675). HPLC purity: 96.29%.

*4.1.9.14. 7-((1-(3,5-dichlorobenzyl)-1H-1,2,3-triazol-4-yl)methoxy)-2-(2,2-dimethyl-2H-chromen-6-yl)chroman-4-one (**10n**).* Yield 58.6% as a yellow oil. ^{1}H NMR (400 MHz, DMSO-d_6, δ): 8.27 (1H, s), 7.70 (1H, d, J = 8.8 Hz), 7.57 (2H, overlap), 7.47 (1H,m), 7.27 (1H, dd, J = 8.2, 2.2 Hz), 7.25 (1H, d, J = 2.2 Hz), 6.77 (1H, d, J = 8.2 Hz), 6.75 (1H, d, J = 2.4 Hz), 6.70 (1H, dd, J = 8.8, 2.4 Hz), 6.42 (1H, d, J = 9.8 Hz), 5.79 (2H, s), 5.78 (1H, d, J = 9.8 Hz), 5.50 (1H, dd, J = 13.1, 2.8 Hz), 5.19 (2H, s), 3.16 (1H, dd, J = 16.8, 13.1 Hz), 2.69 (1H, dd, J = 16.8, 2.8 Hz), 1.38 (6H, s). ^{13}C NMR (100 MHz, DMSO-d_6, δ): 190.7, 164.7, 163.5, 153.1, 142.2, 136.4, 132.2 × 2, 132.0, 131.6, 130.8, 129.5 × 2, 128.5, 128.3, 125.8, 125.5, 122.0, 121.3, 116.2, 115.0, 110.9, 102.3, 79.5, 76.8, 62.0, 49.1, 43.5, 28.2 × 2. ESI-HRMS: m/z 562.1297 $[M+H]^+$ (Calcd for $C_{30}H_{26}Cl_2N_3O_4$, 562.1295). HPLC purity: 91.25%.

*4.1.9.15. 7-((1-(4-bromobenzyl)-1H-1,2,3-triazol-4-yl)methoxy)-2-(2,2-dimethyl-2H-chromen-6-yl)chroman-4-one (**10o**).* Yield 57.6% as a yellow oil. ^{1}H NMR (400 MHz, DMSO-d_6, δ): 8.32 (1H, s), 7.71 (1H, d, J = 8.8 Hz), 7.58 (2H, overlap), 7.28 (3H, overlap), 7.26 (1H, d, J = 2.2 Hz), 6.78 (1H, d, J = 8.1 Hz), 6.76 (1H, d, J = 2.4 Hz), 6.71 (1H, dd, J = 8.8, 2.4 Hz), 6.42 (1H, d, J = 9.8 Hz), 5.79 (1H, d, J = 9.8 Hz), 5.60 (2H, s), 5.51 (1H, dd, J = 13.1, 2.8 Hz), 5.21 (2H, s), 3.18 (1H, dd, J = 16.8, 13.1 Hz), 2.70 (1H, dd, J = 16.8, 2.8 Hz), 1.38 (6H, s). ^{13}C NMR (100 MHz, DMSO-d_6, δ): 190.7, 164.7, 163.5, 153.1, 142.8, 135.8, 132.2 × 2, 132.0, 131.6, 130.7 × 2, 128.5, 128.3, 125.5 × 2, 122.0, 121.9, 121.3, 116.2, 115.1, 110.9, 102.3, 79.5, 76.8, 62.0, 52.6, 43.5, 28.2 × 2. ESI-HRMS: m/z 574.1164 $[M+H]^+$ (Calcd for $C_{30}H_{27}BrN_3O_4$, 574.1161). HPLC purity: 99.28%.

*4.1.9.16. 2-(2,2-dimethyl-2H-chromen-6-yl)-7-((1-(2-fluorobenzyl)-1H-1,2,3-triazol-4-yl)methoxy)chroman-4-one (**10p**).* Yield 57.3% as a yellow oil. ^{1}H NMR (600 MHz, DMSO-d_6, δ): 8.30 (1H, s), 7.72 (1H, d, J = 8.8 Hz), 7.41 (1H, m), 7.36 (1H, m), 7.28–7.20 (4H, overlap), 6.79 (1H, d, J = 8.1 Hz), 6.77 (1H, d, J = 2.4 Hz), 6.72 (1H, dd, J = 8.8, 2.4 Hz), 6.43 (1H, d, J = 9.8 Hz), 5.78 (1H, d, J = 9.8 Hz), 5.69 (2H, s), 5.51 (1H, dd, J = 13.2, 2.8 Hz), 5.22 (2H, s), 3.18 (1H, dd, J = 16.8, 13.2 Hz), 2.70 (1H, dd, J = 16.8, 2.8 Hz), 1.38 (6H, s). ^{13}C NMR (150 MHz, DMSO-d_6, δ): 190.7, 164.8, 163.5, 160.6, 153.1, 142.7, 131.9, 131.6, 131.3, 131.2, 128.5, 128.2, 125.6, 125.5, 125.3, 123.2, 122.0, 121.3, 116.2, 116.0, 115.1, 110.8, 102.3, 79.5, 76.8, 62.0, 47.4, 43.5, 28.2 × 2. ESI-HRMS: m/z 512.1990 $[M+H]^+$ (Calcd for $C_{30}H_{27}FN_3O_4$, 512.1980). HPLC purity: 99.39%.

*4.1.9.17. 2-(2,2-dimethyl-2H-chromen-6-yl)-7-((1-(3-fluorobenzyl)-1H-1,2,3-triazol-4-yl)methoxy)chroman-4-one (**10q**).* Yield 62.3% as a yellow oil. ^{1}H NMR (600 MHz, DMSO-d_6, δ): 8.35 (1H, s), 7.72 (1H, d, J = 8.8 Hz), 7.42 (1H, m), 7.27 (2H, m), 7.17 (3H, m), 6.78 (1H, d, J = 8.1 Hz), 6.77 (1H, d, J = 2.4 Hz), 6.72 (1H, dd, J = 8.8, 2.4 Hz), 6.43 (1H, d, J = 9.8 Hz), 5.79 (1H, d, J = 9.8 Hz), 5.65 (2H, s), 5.51 (1H, dd, J = 13.1, 2.8 Hz), 5.23 (2H, s), 3.19 (1H, dd, J = 16.8, 13.1 Hz), 2.70 (1H, dd, J = 16.8, 2.8 Hz), 1.38 (6H, s). ^{13}C NMR (150 MHz, DMSO-d_6, δ): 190.7, 164.7, 163.5, 162.8, 153.1, 142.1, 139.1, 132.0, 131.6, 131.3, 128.5, 128.3, 125.6, 125.5, 124.5, 122.0, 121.3, 116.2, 115.5, 115.3, 115.1, 110.8, 102.3, 79.5, 76.8, 62.0, 52.6, 43.5, 28.2 × 2. ESI-HRMS: m/z 534.1799 $[M+Na]^+$ (Calcd for $C_{30}H_{26}FN_3O_4Na$, 534.1800). HPLC purity: 95.89%.

*4.1.9.18. 2-(2,2-dimethyl-2H-chromen-6-yl)-7-((1-(4-fluorobenzyl)-1H-1,2,3-triazol-4-yl)methoxy)chroman-4-one (**10r**).* Yield 63.3% as a yellow oil. ^{1}H NMR (600 MHz, DMSO-d_6, δ): 8.31 (1H, s), 7.71 (1H, d, J = 8.8 Hz), 7.45–7.37 (2H, overlap), 7.27 (1H, dd, J = 8.1, 2.3 Hz), 7.25 (1H, d, J = 2.3 Hz), 7.23–7.19 (2H, overlap), 6.78 (1H, d, J = 8.1 Hz), 6.76 (1H, d, J = 2.4 Hz), 6.71 (1H, dd, J = 8.8, 2.4 Hz), 6.43 (1H, d, J = 9.8 Hz), 5.78 (1H, d, J = 9.8 Hz), 5.61 (2H, s), 5.51 (1H, dd, J = 13.1, 2.8 Hz), 5.21 (2H, s), 3.18 (1H, dd, J = 16.8, 13.1 Hz), 2.70 (1H, dd, J = 16.8, 2.8 Hz), 1.38 (6H, s). ^{13}C NMR (150 MHz, DMSO-d_6, δ): 190.7, 164.8, 163.6, 162.4, 153.1, 142.7, 132.7, 132.0, 131.6, 130.9, 130.8, 128.5, 128.3, 125.5, 125.4, 122.0, 121.3, 116.2 × 2, 116.0, 115.1, 110.8, 102.3, 79.5, 76.8, 62.0, 52.5, 43.5, 28.2 × 2. ESI-HRMS: m/z 512.1962 $[M+H]^+$ (Calcd for $C_{30}H_{27}FN_3O_4$, 512.1980). HPLC purity: 99.28%.

*4.1.9.19. 2-(2,2-dimethyl-2H-chromen-6-yl)-7-((1-(4-(trifluoromethyl)benzyl)-1H-1,2,3-triazol-4-yl)methoxy)chroman-4-one (**10s**).* Yield 73.2% as a yellow oil. ^{1}H NMR (600 MHz, DMSO-d_6, δ): 8.37 (1H, s), 7.76 (2H,overlap), 7.72 (1H, d, J = 8.8 Hz), 7.51 (2H,overlap), 7.27 (1H, dd, J = 8.2, 2.3 Hz), 7.25 (1H, d, J = 2.3 Hz), 6.77 (2H, overlap), 6.72 (1H, dd, J = 8.8, 2.4 Hz), 6.43 (1H, d,

J = 9.8 Hz), 5.79 (1H, d, J = 9.8 Hz), 5.75 (2H, s) 5.51 (1H, dd, J = 13.1, 2.8 Hz), 5.22 (2H, s), 3.19 (1H, dd, J = 16.8, 13.1 Hz), 2.70 (1H, dd, J = 16.8, 2.8 Hz), 1.38 (6H, s). ^{13}C NMR (150 MHz, DMSO-d_6, δ): 190.7, 164.7, 163.6, 153.1, 142.8, 141.1, 132.0, 131.6, 129.2 × 2, 129.1, 128.5, 128.3, 126.2 × 2, 125.7, 125.5, 124.6, 122.0, 121.3, 116.2, 115.1, 110.9, 102.3, 79.5, 76.8, 62.0, 52.7, 43.5, 28.2 × 2. ESI-HRMS: m/z 561.1932 $[M+H]^+$ (Calcd for $C_{31}H_{27}F_3N_3O_4$, 561.1931). HPLC purity: 94.42%.

4.2. Biological assays

4.2.1. Cell culture

Huh7 and 293T cells were cultured in Dulbecco's modified Eagle's medium (DMEM, Invitrogen) with 10% fetal bovine serum (FBS, Cell Culture Bioscience), 10 units/mL of penicillin, 10 mg/mL of streptomycin in a humidified 5% CO_2 incubator at 37 °C.

4.2.2. Cytotoxicity assay

1×10^4 of Huh7 cells were seeded per well overnight, treated with compounds for 72 h. The Cell Proliferation Kit II (XTT, Roche Diagnostics, Mannheim, Germany) (The test concentration of all compounds is 100 μg/mL) and CellTiter-Glo® Luminescent Cell Viability Assay (The concentration gradients of compounds **10m** and **10r** are 1 μM, 3 μM, 10 μM, 30 μM, respectively and the test concentration of the positive drug is 10 U/mL.) were used for *in vitro* proliferation assays according to the manufacturer's instructions.

4.2.3. mCherry-NLS-IPS visualization system

The VSV-G, Pol and mCherry-NLS-IPS1 plasmids were transfected into 1×10^7 293T cells according to the method provided by the Trans IT LT1 (Mirus) kit. After 72 h, the supernatant of the culture medium rich in mCherry-NLS-IPS recombinant virus was collected and then filtered through a 0.22 μM filter. Huh7 cells were infected with mCherry-NLS-IPS recombinant virus, and the expression of red fluorescence was observed one week later to determine the establishment of a visualization system [29].

4.2.4. Primary screening

Cells were seeded in 96-well plates at 5×10^4 and cultured overnight. Huh7-mCherry-NLS-IPS cells (multiplicity of infection (MOI) of 1) were infected with the HCV (JFH1). After 6 h, the cells were washed with the medium and cultured by adding a medium containing different compounds, and sobosbuvir was used as a positive medicine. After 72 h of treatment, the change of the fluorescence signal in the cells was observed by using BZ-X710 KEYENCE.

4.2.5. Assay of HCV progeny virus production

Cells were seeded in 96-well plates at 1×10^4 and cultured overnight. Huh7 cells were infected with the HCV (multiplicity of infection (MOI) of 0.1). After 6 h, the virus was washout with medium, following with compounds treatment for 72 h. Then the supernatant was harvested, and used to infect another Huh7 cells. After 48 h, total RNA was extracted and HCV mRNA was determined by RT-PCR.

4.2.6. RNA inhibition (RT-PCR)

For RNA extraction, column purification was performed using RNeasy kit (QIAGEN) according to the manufacturer's protocol. 100 μL of lysis buffer was added to the 96-well plate to lyse the cells. Mix 70% ethanol with the dissolved sample and transfer to the chromatography column. Centrifuge at 10,000 g for 15 s, then discard the waste. The column was washed once with 700 μL of RW1 solution and twice with RPE solution. The column was rotated to 16000 g. 50 μL of elution buffer was added to the column and allowed to stand at room temperature for 1 min. The column was centrifuged at 10,000 g for 1 min, RNA was collected, and the RNA concentration was measured with a Nanodrop (Thermo-Fisher) spectrophotometer. A Thunderbird probe one-step RT-PCR (TOYOBO) kit was used for RNA quantification. The sequence of the front primer (R6-130-S17) used was 5′-CGGGAGAGCCATAGTGG-3′, the sequence of the rear primer (R6-130-R19) was 5′-AGTACCACAAGGCCTTTCG-3′, and the TaqMan probe (R6-148-S21FT) was FAM-5′-CTGCGGAACCGGTGAGTACAC-3′ TAMRA. Use the StepOnePlus real-time PCR biosystems for quantitative analysis.

4.2.7. Western blot analysis

Cells were lysed with RIPA buffer (25 mM Tris-HCl [pH 7.6], 150 mM NaCl, 1% NP-40, 1% sodium deoxycholate, 0.1% SDS). Laemmli buffer (4% SDS, 20% glycerin, 10% 2-mercaptoethanol, 0.004% bromophenol blue and 0.125 M tris-HCl [pH 6.8]) was then added to the sample and heated for 10 min at 95 °C. It was left to stand for 5 min at 4 °C. The membranes were blocked with 1% skim milk solution and probed with a primary antibody (GAPDH, sigma, 1/1000; NS3, 1/1000 and Core Ab, 1/3000, National Institute of Infectious Diseases) followed by the corresponding secondary antibody (Anti-mouse IgG-conjugated HRP, cell signal, 1/5000 and anti-rabbit IgG-conjugated HRP, cell signal, 1/5000). The PVDF membrane was treated with a developer (GE health-care) and detected using a chemiluminescence detection instrument LAS-3000 (Fujifilm). ImageQuant LAS 4000 was used for detection and analysis.

4.2.8. HCV pseudovirus entry assay

HCVpp entry assay was performed as described [42]. After treated 5×10^3 Huh-7 cells/well in a 96-well plate with compounds for 24 h, cells were infected with HCVpp. After 6 h infection, virus and compounds were washed out. Bright-Glo reagent (Promega) and Lumat LB 9507 was performed for luciferase activity 48 h later.

For wildtype entry assay, cells were pre-treated with compounds for 24 h then compounds were washed out. Cells were infected with the HCV (multiplicity of infection (MOI) of 0.1) for 6 h. RT-PCR was performed to detect HCV wildtype RNA 48 h later.

Declaration of competing interest

The authors declare that they have no known competing financial interests or personal relationships that could have appeared to influence the work reported in this paper.

Acknowledgments

The authors are very grateful to the support of the China Natural Science Foundation (81872766), Key R & D projects of Liaoning Province, China (2020JH2/10300058), the Young and Middle-aged Science and Technology Innovative Talent Support Program of Shenyang City (RC180250). This study was also supported by a grant from the Research Program on Hepatitis from the Japan Agency for Medical Research and Development (20fk0210053j0002). We are very much appreciated Dr. Fukuhara in Hokkaido University and Dr. Matsuura in Osaka University for providing us the mCherry-NLS-IPS1 reporter system.

Appendix A. Supplementary data

Supplementary data to this article can be found online at https://doi.org/10.1016/j.ejmech.2021.113395.

References

[1] M. Cesare, D.M. Luigino, M. Endri, V. Marcella, T. Maurizio, G. Valter, A. Pietro, P. Gabriele, Hepatitis C virus- related cryoglobulinemic vasculitis: a review of the role of the new direct antiviral agents (DAAs) therapy, Autoimmun. Rev. 19 (2020) 102589, https://doi.org/10.1016/j.autrev.2020.102589.

[2] C.H. Tseng, C.K. Lin, Y.L. Chen, C.K. Tseng, J.Y. Lee, J.C. Lee, Discovery of naphtho [1,2-d]oxazole derivatives as potential anti-HCV agents through inducing heme oxygenase-1 expression, Eur. J. Med. Chem. 143 (2018) 970–982, https://doi.org/10.1016/j.ejmech.2017.12.006.

[3] A. Rosenquist, B. Samuelsson, P.O. Johansson, M.D. Cummings, O. Lenz, P. Raboisson, K. Simmen, S. Vendeville, H. de Kock, M. Nilsson, A. Horvath, R. Kalmeijer, G. de la Rosa, M. Beumont-Mauviel, Discovery and development of simeprevir (TMC435), a HCV NS3/4A protease inhibitor, J. Med. Chem. 57 (2014) 1673–1693, https://doi.org/10.1021/jm401507s.

[4] C.Q. Lim, K. George, W. Amy J, O. Lacy R, B. Daniel W, H. Michael, Isolation of a cDNA clone derived from a blood-borne non-A, non-B viral hepatitis genome, Science 244 (1989) 359–362, https://doi.org/10.1126/science.2523562.

[5] M.P. Manns, M. Buti, E. Gane, J.M. Pawlotsky, H. Razavi, N. Terrault, Z. Younossi, Hepatitis C virus infection, Nat. Rev. Dis. Primers 3 (2017) 17006, https://doi.org/10.1038/nrdp.2017.6.

[6] J. L Kim, K. A Morgenstern, C. Lin, T. Fox, M. D Dwyer, J.A. Landro, S. P Chambers, W. Markland, C.A. Lepre, E. T O'Malley, S. L Harbeson, C. M Rice, M.A. Murcko, P. R Caron, J.A. Thomson, Crystal structure of the hepatitis C virus NS3 protease domain complexed with a synthetic NS4A cofactor peptide, Cell 87 (1996) 343–355, https://doi.org/10.1016/S0092-8674(00)81351-3.

[7] H.T.L. Tran, K. Morikawa, F. Penin, M. Quadroni, J. Gouttenoire1, D. Moradpour, Hepatitis C virus NS3-4A protease targets the host factor BNIP1 at a non-canonical cleavage site, J. Hepatol. 62 (2015) S263–S864, https://doi.org/10.1016/S0168-8278(15)30886-2.

[8] M. David R, M. Takahiro, L. William, H. Chris, S.B. Susanne, G. Brent, Protease inhibitors block multiple functions of the NS3/4A protease-helicase during the hepatitis C virus life cycle, J. Virol. 89 (2015) 5362–5370, https://doi.org/10.1128/JVI.03188-14.

[9] C. Roh, S.K. Jo, (-)-Epigallocatechin gallate inhibits hepatitis C virus (HCV) viral protein NS5B, Talanta 85 (2011) 2639–2642, https://doi.org/10.1016/j.talanta.2011.08.035.

[10] F.B. Akher, A. Farrokhzadeh, P. Ramharack, L. Shunmugam, F.R. Van Heerden, M.E.S. Soliman, Discovery of novel natural flavonoids as potent antiviral candidates against hepatitis C virus NS5B polymerase, Med. Hypotheses 132 (2019) 109359, https://doi.org/10.1016/j.mehy.2019.109359.

[11] A. Rojas, J.A. Del Campo, S. Clement, M. Lemasson, M. Garcia-Valdecasas, A. Gil-Gomez, I. Ranchal, B. Bartosch, J.D. Bautista, A.R. Rosenberg, F. Negro, M. Romero-Gomez, Effect of quercetin on hepatitis C virus life cycle: from viral to host targets, Sci. Rep. 6 (2016) 31777, https://doi.org/10.1038/srep31777.

[12] J.F. Shimizu, C.S. Lima, C.M. Pereira, C. Bittar, M.N. Batista, A.C. Nazare, C.R. Polaquini, C. Zothner, M. Harris, P. Rahal, L.O. Regasini, A.C.G. Jardim, Flavonoids from pterogyne nitens inhibit hepatitis C virus entry, Sci. Rep. 7 (2017) 1–9, https://doi.org/10.1038/s41598-017-16336-y.

[13] R. Khachatoorian, V. Arumugaswami, S. Raychaudhuri, G.K. Yeh, E.M. Maloney, J. Wang, A. Dasgupta, S.W. French, Divergent antiviral effects of bioflavonoids on the hepatitis C virus life cycle, Virology 433 (2012) 346–355, https://doi.org/10.1016/j.virol.2012.08.029.

[14] B. Dinda, S. Dinda, S. DasSharma, R. Banik, A. Chakraborty, M. Dinda, Therapeutic potentials of baicalin and its aglycone, baicalein against inflammatory disorders, Eur. J. Med. Chem. 131 (2017) 68–80, https://doi.org/10.1016/j.ejmech.2017.03.004.

[15] N. Ren, P. Liu, S. Nie, X.J. Zhang, M.D. Chen, Effect of flavonoids on the essential elements in liver and kidney of rats exposed to aluminum, Trace Elem. Electrolytes 36 (2019) 197–203, https://doi.org/10.5414/tex01586.

[16] M. Boozari, S. Soltani, M. Iranshahi, Biologically active prenylated flavonoids from the genus *Sophora* and their structure-activity relationship-A review, Phytother Res. 33 (2019) 546–560, https://doi.org/10.1002/ptr.6265.

[17] S. Karel, Cytotoxic potential of C-prenylated flavonoids, Phytochemistry Rev. 13 (2014) 245–275, https://doi.org/10.1007/s11101-013-9308-2.

[18] Q. Sun, D. Wang, F.F. Li, G.D. Yao, X. Li, L.Z. Li, X.X. Huang, S.J. Song, Cytotoxic prenylated flavones from the stem and root bark of *Daphne giraldii*, Bioorg. Med. Chem. Lett 26 (2016) 3968–3972, https://doi.org/10.1016/j.bmcl.2016.07.002.

[19] B. Yang, J.L. Yang, Y.P. Zhao, H.L. Liu, Y.M. Jiang, The plant resources, structure characteristics, biological activities and synthesis of pyranoflavonoids, Curr. Med. Chem. 23 (2016) 3078–3115. https://10.2174/0929867323666160510123147.

[20] S. Zhang, Z. Xu, C. Gao, Q.C. Ren, L. Chang, Z.S. Lv, L.S. Feng, Triazole derivatives and their anti-tubercular activity, Eur. J. Med. Chem. 138 (2017) 501–513, https://doi.org/10.1016/j.ejmech.2017.06.051.

[21] P. Shanmugavelan, S. Nagarajan, M. Sathishkumar, A. Ponnuswamy, P. Yogeeswari, D. Sriram, Efficient synthesis and in vitro antitubercular activity of 1,2,3-triazoles as inhibitors of Mycobacterium tuberculosis, Bioorg. Med. Chem. Lett 21 (2011) 7273–7276, https://doi.org/10.1016/j.bmcl.2011.10.048.

[22] M. Gholampour, S. Ranjbar, N. Edraki, M. Mohabbati, O. Firuzi, M. Khoshneviszadeh, Click chemistry-assisted synthesis of novel amino-naphthoquinone-1,2,3-triazole hybrids and investigation of their cytotoxicity and cancer cell cycle alterations, Bioorg. Chem. 88 (2019) 102967, https://doi.org/10.1016/j.bioorg.2019.102967.

[23] D. Dheer, V. Singh, R. Shankar, Medicinal attributes of 1,2,3-triazoles: current developments, Bioorg. Chem. 71 (2017) 30–54, https://doi.org/10.1016/j.bioorg.2017.01.010.

[24] P. Cikla-Suzgun, N. Kaushik-Basu, A. Basu, P. Arora, T.T. Talele, I. Durmaz, R. Cetin-Atalay, S.G. Kucukguzel, Anti-cancer and anti-hepatitis C virus NS5B polymerase activity of etodolac 1,2,4-triazoles, J. Enzym. Inhib. Med. Chem. 30 (2015) 778–785, https://doi.org/10.3109/14756366.2014.971780.

[25] M. Hamada, V. Roy, T.R. McBrayer, T. Whitaker, C. Urbina-Blanco, S.P. Nolan, J. Balzarini, R. Snoeck, G. Andrei, R.F. Schinazi, L.A. Agrofoglio, Synthesis and broad spectrum antiviral evaluation of bis(POM) prodrugs of novel acyclic nucleosides, Eur. J. Med. Chem. 67 (2013) 398–408, https://doi.org/10.1016/j.ejmech.2013.06.053.

[26] W.H. Song, M.M. Liu, D.W. Zhong, Y.L. Zhu, M. Bosscher, L. Zhou, D.Y. Ye, Z.H. Yuan, Tetrazole and triazole as bioisosteres of carboxylic acid: discovery of diketo tetrazoles and diketo triazoles as anti-HCV agents, Bioorg. Med. Chem. Lett 23 (2013) 4528–4531, https://doi.org/10.1016/j.bmcl.2013.06.045.

[27] B.G. Youssif, Y.A. Mohamed, M.T. Salim, F. Inagaki, C. Mukai, H.H. Abdu-Allah, Synthesis of some benzimidazole derivatives endowed with 1,2,3-triazole as potential inhibitors of hepatitis C virus, Acta Pharm. 66 (2016) 219–231, https://doi.org/10.1515/acph-2016-0014.

[28] G.V. Rao, B.N. Swamy, V. Chandregowda, G.C. Reddy, Synthesis of (+/-)Abyssinone I and related compounds: their anti-oxidant and cytotoxic activities, Eur. J. Med. Chem. 44 (2009) 2239–2245, https://doi.org/10.1016/j.ejmech.2008.05.032.

[29] G. Zhang, S. Liu, W. Tan, R. Verma, Y. Chen, D. Sun, Y. Huan, Q. Jiang, X. Wang, N. Wang, Y. Xu, C. Wong, Z. Shen, R. Deng, J. Liu, Y. Zhang, W. Fang, Synthesis and biological evaluations of chalcones, flavones and chromenes as farnesoid x receptor (FXR) antagonists, Eur. J. Med. Chem. 129 (2017) 303–309, https://doi.org/10.1016/j.ejmech.2017.02.037.

[30] Y.M. Loo, D.M. Owen, K. Li, A.K. Erickson, C.L. Johnson, P.M. Fish, D.S. Carney, T. Wang, H. Ishida, M. Yoneyama, T. Fujita, T. Saito, W.M. Lee, C.H. Hagedorn, D.T. Lau, S.A. Weinman, S.M. Lemon, M. Gale Jr., Viral and therapeutic control of IFN-beta promoter stimulator 1 during hepatitis C virus infection, Proc. Natl. Acad. Sci. U. S. A. 103 (2006) 6001–6006, https://doi.org/10.1073/pnas.0601523103.

[31] H. Mori, T. Fukuhara, C. Ono, T. Tamura, A. Sato, Y. Fauzyah, M. Wada, T. Okamoto, T. Noda, T. Yoshimori, Y. Matsuura, Induction of selective autophagy in cells replicating hepatitis C virus genome, J. Gen. Virol. 99 (2018) 1643–1657, https://doi.org/10.1099/jgv.0.001161.

[32] N. Ishii, K. Watashi, T. Hishiki, K. Goto, D. Inoue, M. Hijikata, T. Wakita, N. Kato, K. Shimotohno, Diverse effects of cyclosporine on hepatitis C virus strain replication, J. Virol. 80 (2006) 4510–4520, https://doi.org/10.1128/JVI.80.9.4510-4520.2006.

[33] H. Ohashi, K. Nishioka, S. Nakajima, S. Kim, R. Suzuki, H. Aizaki, M. Fukasawa, S. Kamisuki, F. Sugawara, N. Ohtani, M. Muramatsu, T. Wakita, K. Watashi, The aryl hydrocarbon receptor-cytochrome P450 1A1 pathway controls lipid accumulation and enhances the permissiveness for hepatitis C virus assembly, J. Biol. Chem. 293 (2018) 19559–19571, https://doi.org/10.1074/jbc.ra118.005033.

[34] L.T. Lin, R.S. Noyce, T.N. Pham, J.A. Wilson, G.R. Sisson, T.I. Michalak, K.L. Mossman, C.D. Richardson, Replication of subgenomic hepatitis C virus replicons in mouse fibroblasts is facilitated by deletion of interferon regulatory factor 3 and expression of liver-specific microRNA 122, J. Virol. 84 (2010) 9170–9180, https://doi.org/10.1128/JVI.00559-10.

[35] T. Kato, T. Date, M. Miyamoto, M. Sugiyama, Y. Tanaka, E. Orito, T. Ohno, K. Sugihara, I. Hasegawa, K. Fujiwara, K. Ito, A. Ozasa, M. Mizokami, T. Wakita, Detection of anti-hepatitis C virus effects of interferon and ribavirin by a sensitive replicon system, J. Clin. Microbiol. 43 (2005) 5679–5684, https://doi.org/10.1128/JCM.43.11.5679-5684.2005.

[36] K. Fukano, S. Tsukuda, M. Oshima, R. Suzuki, H. Aizaki, M. Ohki, S.Y. Park, M. Muramatsu, T. Wakita, C. Sureau, Y. Ogasawara, K. Watashi, Troglitazone impedes the oligomerization of sodium taurocholate cotransporting polypeptide and entry of hepatitis B virus into hepatocytes, Front. Microbiol. 9 (2018) 3257, https://doi.org/10.3389/fmicb.2018.03257.

[37] R. Suzuki, K. Saito, T. Kato, M. Shirakura, D. Akazawa, K. Ishii, H. Aizaki, Y. Kanegae, Y. Matsuura, I. Saito, T. Wakita, T. Suzuki, *Trans*-complemented hepatitis C virus particles as a versatile tool for study of virus assembly and infection, Virology 432 (2012) 29–38, https://doi.org/10.1016/j.virol.2012.05.033.

[38] X.J. Qian, Y.Z. Zhu, P. Zhao, Z.T. Qi, Entry inhibitors: new advances in HCV treatment, Emerg. Microb. Infect. 5 (2016) e3, https://doi.org/10.1038/emi.2016.3.

[39] C.C. Colpitts, T.F. Baumert, Hepatitis C virus cell entry: a target for novel antiviral strategies to address limitations of direct acting antivirals, Hepatol Int 10 (2016) 741–748, https://doi.org/10.1007/s12072-016-9724-7.

[40] F. Xiao, I. Fofana, C. Thumann, L. Mailly, R. Alles, E. Robinet, N. Meyer, M. Schaeffer, F. Habersetzer, M. Doffoel, P. Leyssen, J. Neyts, M.B. Zeisel,

T.F. Baumert, Synergy of entry inhibitors with direct-acting antivirals uncovers novel combinations for prevention and treatment of hepatitis C, Gut 64 (2015) 483–494, https://doi.org/10.1136/gutjnl-2013-306155.
[41] P. Padmanabhan, N.M. Dixit, Modeling suggests a mechanism of synergy between hepatitis C virus entry inhibitors and drugs of other classes, CPT Pharmacometrics Syst. Pharmacol. 4 (2015) 445–453, https://doi.org/10.1002/psp4.12005.
[42] B. Bartosch, J. Dubuisson, F.L. Cosset, Infectious hepatitis C virus pseudoparticles containing functional E1-E2 envelope protein complexes, J. Exp. Med. 197 (2003) 633–642, https://doi.org/10.1084/jem.20021756.